Plant Growth Regul (2017) 83:489–500
DOI 10.1007/s10725-017-0314-z

ORIGINAL PAPER

PnF3H, a flavanone 3-hydroxylase from the Antarctic moss *Pohlia nutans*, confers tolerance to salt stress and ABA treatment in transgenic *Arabidopsis*

Chengcheng Li[1,3] · Shenghao Liu[2] · Xinghao Yao[1,3] · Jing Wang[1] · Tailin Wang[1,3] · Zhaohui Zhang[2] · Pengying Zhang[1,3] · Kaoshan Chen[1,3]

Received: 15 February 2017 / Accepted: 18 August 2017 / Published online: 8 September 2017

Abstract Flavonoids are widely distributed secondary metabolites in plants. However, far less research has been carried out on genes involved in the flavonoid biosynthetic pathways in bryophytes. Here, a novel flavanone 3-hydroxylase gene (*PnF3H*) was cloned from Antarctic moss *Pohlia nutans*. Subcellular localization revealed that PnF3H were mainly distributed to cytosol. The expression of *PnF3H* was rapidly induced by salt, UV-B, cold and drought stresses as well as by exogenously applied abscisic acid (ABA). Transgenic *Arabidopsis* plants of overexpressing *PnF3H* exhibited enhanced tolerance to salt and oxidative stresses. The expression levels of several stress resistance genes (i.e., *AtSOS3, AtP5CS1, AtHKT1, AtCAT1* and *AtAPX1*) were markedly up-regulated in transgenic plants. The activities of antioxidant enzymes were increased, while the content of hydrogen peroxide was obviously decreased in *PnF3H* transgenic plants. Meanwhile, the expression levels of ABA-responsive genes which confer for controlling seeds germination, such as *AtABI4, AtABI5, AtABI3* and *AtABF3* were markedly decreased. Additionally, overexpressing *PnF3H* alleviated the inhibitory effects of naringenin on plant growth and changed the flavonoid components in transgenic plants. Therefore, we proposed that PnF3H was a flavanone 3-hydroxylase involving in regulating the salinity tolerance and ABA sensitivity to enable *P. nutans* to adapt to polar climates.

Keywords Antarctic moss · Flavonoids · Flavanone 3-hydroxylase · Phenotype · Salt stress

Introduction

Flavonoids, a large group of plant secondary metabolites, have abundant biological functions, such as defense against phytopathogens and stress protection. They are found primarily in fruit, grains, bark, vegetables, roots, flowers, tea, wine and stems (Sankari et al. 2014). The basic structure of flavonoids consists of 15 carbon atoms, two benzene rings joined by a linear three-carbon chain. More than 6000 naturally occurring flavonoids have been identified in various plants (Czemmel et al. 2012; Perez-Cano and Castell 2016). These flavonoids can be classified into six classes: flavonols, flavones, isoflavones, flavanones, flavanols and anthocyanidins. Flavonoids have diverse biological functions, including protection against ultraviolet (UV) radiation and phytopathogens, signaling during nodulation, male fertility, auxin transport, as well as the coloration of flowers as a visual signal that attract spollinators (Ferreyra et al. 2012). Moreover, they provide abundant resources for agents that promote and maintain health (Sankari et al. 2014).

Flavonoids are synthesized through the phenylpropanoid pathway, transforming phenylalanine into 4-coumaroyl-CoA, which finally enters the flavonoid biosynthesis pathway (Ferreyra et al. 2012; Li et al. 2017). Flavanone 3-hydroxylase (F3H) is the third enzyme of the central flavonoid

Electronic supplementary material The online version of this article (doi:10.1007/s10725-017-0314-z) contains supplementary material, which is available to authorized users.

✉ Pengying Zhang
zhangpy80@sdu.edu.cn

[1] National Glycoengineering Research Center and School of Life Science, Shandong University, Jinan 250100, China

[2] Marine Ecology Research Center, The First Institute of Oceanography, State Oceanic Administration, Qingdao 266061, China

[3] Shandong Provincial Key Laboratory of Carbohydrate Chemistry and Glycobiology, Jinan 250100, China

biosynthetic pathway, catalyzing the 3-hydroxylation of (2*S*)-flavanones such as naringenin to dihydroflavonols. For example, F3H serves as the intermediate for the biosynthesis of flavan-3-ols in *Reaumuria soongorica* (Liu et al. 2013a). The high expression of *CtF3H* in quinochalcone-type safflower line is associated with the accumulation of quinochalcones and flavonols (Tu et al. 2016). In *Artemisia annua*, the *F3H* transcripts are found to be accumulated in the cultivar with higher level of flavonoids (Xiong et al. 2016). Furthermore, flavonoids and their related key enzymes play an important role in response to diverse biotic and abiotic stresses. Flavonols are increased in *Ligustrum vulgare* under salinity or UV radiation stress and have a significant antioxidant function in plant photoprotection (Agati et al. 2011). In a desert plant *Reaumuria soongorica*, the F3H gene (i.e., *RsF3H*) involves in the flavonoid biosynthesis pathway in response to UV-B radiation and drought stress (Liu et al. 2013a). Overexpression of a tea F3H gene (i.e., *CsF3H*) increases the content of flavan-3-ols in tobacco and confers tolerance to salt stress and fungus *Alternaria solani* infection (Mahajan and Yadav 2014). Overexpression of a tomato F3H-like gene (i.e., *SlF3HL*) stimulates flavonoid biosynthesis and improves chilling tolerance in tobacco (Meng et al. 2015). However, there is still no report about the roles of F3H in bryophytes to stress responses.

In Antarctica continent, high salt, low temperatures, extreme dryness and high radiation are the major constraints to plant growth. The moss flora constitutes the predominant terrestrial vegetation in ice-free coastal regions of Antarctica (Skotnicki et al. 2004). Mosses have evolved a variety of mechanisms to cope with the extreme environment of Antarctica. For example, Antarctic cryptogams resist the effects of UV radiation using efficient systems that repair damages by synthesizing compounds such as UV-B-absorbing pigments and anthocyanins (Singh et al. 2010). The moss *Bryum argenteum* can tolerate the high-intensity light by producing abundant xanthophyll cycle pigments (Schroeter et al. 2012). Furthermore, several cell wall-bound insoluble phenylpropanoids function in relatively passive UV-screening processes that increase the tolerance to UV radiation (Clarke and Robinson 2008). However, the underlying mechanisms that enable Antarctic mosses to survive under extreme conditions have not been characterized as completely as the corresponding processes of vascular plants such as *Arabidopsis thaliana* and rice.

To clarify the mechanism regulating stress acclimation, we previously conducted a transcript-level investigation of an Antarctic moss (i.e., *Pohlia nutans*) exposed to cold stress using Illumina high-throughput sequencing technology (Liu et al. 2013b). We also found that several receptor-like kinases (RLK) from *Pohlia nutans* serve in high salinity (Wang et al. 2016) and ROS scavenging (Zhang et al. 2014), and provide protection against chilling-stress tolerance (Liu et al. 2017), involving in the adaptation of Antarctic moss to the polar environment. In this paper, we cloned a novel F3H gene (i.e., *PnF3H*) from the Antarctic moss *P. nutans* and studied its role in plant salt stress resistance. We proposed that PnF3H may serve as a flavonoid biosynthetic enzyme, conferring the salinity tolerance in the Antarctic moss *P. nutans*.

Materials and methods

Plant materials and stress treatments

We collected the Antarctic moss *Pohlia nutans* from the terrane near the Great Wall Station on King George Island during the 31th CHINARE in March 2014. Mosses were cultivated in flowerpots containing a mixture of Base Substrate (Klasmann–Deilmann, Geeste, Germany) and local soil (1:1) (Liu et al. 2017). They were incubated at 16 °C and 70% relative humidity, under 70 μmol photons m^{-2} s^{-1} light. Mosses cultivated under above conditions were used as controls in all experiments. For cold treatments, mosses were kept in 4 °C for 0, 1, 3, 6, 12, or 24 h. For NaCl and ABA treatment, mosses were sprayed with 200 mM NaCl or 50 μM ABA, respectively, and incubated for 0, 0.5, 1, 3, 6, or 12 h. For the mock osmotic stress and UV-B radiation stress, mosses were treated with 20% (w/v) polyethylene glycol 6000 solution or transferred under an 8 W UV-B lamp (302 nm, 70 μW cm^{-2} irradiance), respectively, for 0, 0.5, 1, 3, 6, or 12 h. The samples were immediately frozen in liquid nitrogen after various stress treatments.

Reverse transcription-PCR and real-time PCR analyses

Total RNA was extracted using CTAB method (Zhang et al. 2014). The CTAB buffer contained 2% cetyltrimethylammonium bromide, 1% polyvinylpyrrolidone K-30, 100 mM Tris–HCl (pH8.0), 20 mM EDTA, 1.4 M NaCl, 0.5 g L^{-1} spermidine, and 2% β-mercaptoethanol (added just before use). Moss gametophyte tissues or *A. thaliana* seeds 2 days after germination with NaCl and ABA treatment were used for total RNA isolation. cDNA was synthesized from 0.5 μg total RNA using the 5× All-In-One RT MasterMix Kit (Abm, Canada). Real-time PCR assays were conducted using the Bestar SybrGreen qPCR Master Mix (DBI Bioscience, Shanghai, China). The PCR reaction consists of a 2 min denaturation at 95 °C, followed by 40 cycles of 95 °C/20 s, 58 °C/20 s, and 72 °C/20 s, completed by an extension step of 10 min at 72 °C. All reactions were completed in triplicate. Data were analyzed using the $2^{-\Delta\Delta Ct}$ method (Livak and Schmittgen 2001).

Bioinformatic analysis of PnF3H sequence

The *Arabidopsis* F3H protein (GenBank Acc. Q9S818) was used to blast against the *P. nutans* transcriptome (Liu et al. 2013b). Then, a flavanone 3-hydroxylase protein (i.e., PnF3H) with 356 Amino acids were identified from *P. nutans*. The ClustalW software was used for multiple sequences alignments between PnF3H and other plant F3Hs. To construct the phylogenetic tree, a neighbor-joining (NJ) method was adopted within ClustalX and MEGA4.0 software (Kumar et al. 2008). Meanwhile, the 3-D structure analysis of PnF3H was performed using the SWISS-MODEL program (Biasini et al. 2014), while PyMol software was used to visualize and manipulate structural models.

Subcellular localization of PnF3H

To construct the *p35S::PnF3H::green fluorescent protein (GFP)* plasmid, the full-length sequence of *PnF3H* was amplified and inserted into a modified pBI221 vector. The gene-specific PCR primers were listed in Table S1. Subcellular localization was performed using a polyethylene glycol 4000-mediated protoplast transformation method (Liu et al. 2017). Briefly, 4×10^4 mesophyll protoplasts isolated from 4-week-old *A. thaliana* Col-0 seedlings were transformed with 10 μg *p35S::PnF3H::GFP*/pBI221 vector. The GFP signal and chlorophyll autofluorescence were detected by a confocal laser-scanning microscope (LSM700, Carl Zeiss).

Construction of PnF3H transgenic *Arabidopsis*

PnF3H was amplified using the gene-specific primers listed in Table S1. The PCR procedure comprised of 3 min denaturation at 95 °C, followed by 34 cycles of 94 °C for 30 s, 57 °C for 30 s, 72 °C for 60 s, with a final reaction of 72 °C for 10 min. The PCR product was inserted into *Xba* I and *Kpn* I sites of a modified pROK2 vector containing a CaMV35S promoter. Then, the *CaMV35S::PnF3H*/pROK2 vector was introduced into *Arabidopsis* Col-0 plants using an *Agrobacterium tumefaciens*-mediated floral dip method (Zhang et al. 2006). Homozygous transgenic segregates were selected on 1/2 Murashige and Skoog (MS) medium supplemented with 50 μg mL^{-1} kanamycin. At last, three *PnF3H*-overexpressing transgenic *Arabidopsis* lines (i.e., AtOE1, AtOE2, and AtOE3) from the T_3 generation were selected for phenotypic analysis. The expression levels of *PnF3H* in AtOE plants were detected by RT-PCR.

Arabidopsis treatment and phenotype assay

For seed germination assay, surface-sterilized seeds were plated on 1/2 MS agar medium supplemented with 0, 100 or 125 mM NaCl, with 0, 0.5, or 0.75 μM ABA. Seeds were held in darkness at 4 °C for 2 days to break dormancy, and subsequently were cultured under a 16-h light/8-h dark photoperiod at 22 °C for 4–6 days. Seed germination rates were calculated by counting the proportion of the WT plants and the AtOE lines bearing open cotyledons (Zhang et al. 2014; Wang et al. 2016). For root length assays, seeds were sown on 1/2 MS agar medium with NaCl, ABA and H_2O_2, and held in darkness at 4 °C for 2 days to break dormancy, and then kept the plates upright in 16-h light/8-h dark photoperiod at 22 °C for 3 days (Yu et al. 2017).

Measurement of the ROS level and the activities of antioxidant enzymes

ROS level was detected by DAB staining as described previously (Wang et al. 2016). 2-week-old wild type and transgenic plants were treatment with 200 mM NaCl for 24 h or not. Then leaves were detached and infiltrated in 1 mg mL^{-1} DAB with 10 mM sodium phosphate buffer (pH 3.8) overnight in dark. These stained leaves were decolorized by boiling in 95% ethanol solution. Finally, the staining samples were photographed. For antioxidant enzymes activities, 2-week-old *Arabidopsis* seedlings were treated by 200 mM NaCl for 24 h. Whole seedlings (0.5 g) were ground in an ice-cold mortar in the 5 mL homogenization buffer (50 mM potassium phosphate, pH 7.4). Supernatants were used to determine the activities of ROS-scavenging enzymes (Meng et al. 2015; Chen et al. 2017). Finally, the absorbance value of reaction mixtures was measured at 560 and 240 nm, respectively.

Measurement of ABA by LC–ESI–MS/MS system

Plant materials (100 mg fresh weight) were frozen in liquid nitrogen, ground into powder, and extracted with 1 mL methanol containing 20% water at 4 °C for 12 h. The extract was centrifuged at 12,000×*g* under 4 °C for 15 min. The supernatant was collected and then evaporated to dryness under nitrogen gas stream, reconstituted in 100 mL acetonitrile containing 5% water. The solution was centrifuged and the supernatant were analyzed using an LC–ESI–MS/MS system as previously described (Fu et al. 2012; Chen et al. 2013). The analytical conditions were as follows, HPLC: column, Waters ACQUITY UPLC HSS T3 C18 (1.8 μm, 2.1 mm × 100 mm); solvent system, water (0.04% acetic acid):acetonitrile (0.04% acetic acid); gradient program, 100:0 V/V at 0 min, 5:95 V/V at 11.0 min, 5:95 V/V at 12.0 min, 95:5 V/V at 12.1 min, 95:5 V/V at 15.0 min; flow rate, 0.40 mL min^{-1}; temperature, 40 °C; injection volume: 5 μL. The effluent was alternatively connected to an ESI-triple quadrupole-linear ion trap (Q TRAP)-MS.

Naringenin-feeding experiments and flavonoid metabolism profiling by HPLC analysis

Surface-sterilized seeds (3 mg) of wild-type and transgenic *Arabidopsis* were cultured in 100 mL of liquid MS medium (Murashige and Skoog plant salt mixture, Gamborg's B5 vitamin salt mixture, 1% sucrose, 0.05% MES, pH 5.7) under long-day conditions for 2 weeks with or without 200 μM naringenin. Then seedlings were washed with distilled water three times, frozen in liquid nitrogen (Yun et al. 2008). Frozen *Arabidopsis* seedlings were freeze-dried for 48 h and were fully ground to powder. The dried powder (0.5 g) was mixed with 1 mL extraction solvent (70% HPLC-grade methanol with 0.1% HPLC-grade formic acid) and then sonicated in an ultrasonic water bath at room temperature for 1 h. The samples were placed at 4 °C overnight. The following day, the resulting extract was centrifuged at 12,000 rpm for 20 min at 4 °C. The supernatant was then filtered through Millipore filter (0.45 μm) prior to injection in HPLC. For HPLC analysis, 10 μL of the filtrate was performed with reversed-phase HPLC (Shimadzu LC-20A, Japan) coupled to an PDA detector on a Agilent C18 column (4.6×250 mm, 5 μm), mobile phases were H_2O (A) and acetonitrile (B), and the elution program was: 0–30 min, 30% B-80% B; 30–35 min, 80% B; 35–45 min, 30% B. The flow rate of the mobile phase was 0.8 mL min^{-1}, the temperature of the column was set at 30 °C, the elution was monitored by the absorption profile at 280 nm (Mahajan and Yadav 2014; Xiong et al. 2016).

Results

Multiple sequence alignment and phylogenetic analysis

The full-length of *PnF3H* cDNA from *Pohlia nutans* was 1072 bp, encoding a 356-amino-acid protein with a predicted molecular weight of 39.10 kDa and an isoelectric point of 6.22. Multiple sequence alignment analysis indicated that PnF3H is homologous with other F3Hs from species such as *Physcomitrella patens* subsp. *patens* (Pp1s287_51), *Arabidopsis thaliana* (AT3G51240), *Elaeis guineensis* (XP_0109225), *Erythranthe guttata* (XP_0128321), *Medicago truncatula* (XP_0134491) (Fig. 1a). Like other members of 2OG-Fe^{II}_Oxy dioxygenase family, PnF3H contained the conserved domains: the highly conserved ferrous iron binding site HXDX55H (labeled red box) and the 2-oxoglutarate (2-ODD) binding domain RXS (Arg301 and Ser303) (Fig. 1a). Homology modeling of PnF3H was carried out using the SWISS-MODEL program, and RXS motif and ferrous iron binding site were presented in Fig. 1h. Phylogenic analysis showed that PnF3H was clustered more closely with F3Hs from other species other than with anthocyanidin synthase (ANS) or flavonol synthase (FLS) (Fig. 1b).

PnF3H transcription level of multiple abiotic stresses

The *PnF3H* transcript profiles under various abiotic stress conditions were uncovered by Real-time PCR analysis. The *PnF3H* expression levels increased by 2.75-fold at 0.5 h after the 200 mM NaCl treatment and remained high up to 12 h after treatment (Fig. 1c). Similarly, the *PnF3H* expression levels increased by 2.49-fold at 1 h and then slightly decreased to 1.47-fold at 24 h with cold treatment (Fig. 1d). For the simulated drought stress (i.e., 20% polyethylene glycol 6000), the *PnF3H* expression levels enhanced by 2.39-fold at 3 h and the transcript abundance remained high up to 12 h (Fig. 1e). In the UV-B radiation, the *PnF3H* expression levels increased and reached the maximum level of 4.57-fold at 3 h (Fig. 1f). After exogenous ABA treatment, the *PnF3H* expression levels increased quickly and reached the maximum level of 2.57-fold at 0.5 h (Fig. 1g). Thus, *PnF3H* transcripts were induced by various stress and may play a positive role in stress tolerance.

Subcellular localization of PnF3H in *Arabidopsis* mesophyll protoplasts

To investigate the protein subcellular localization, PnF3H-GFP fusion proteins were transiently expressed in *Arabidopsis* mesophyll protoplasts. In *p35S::GFP*/pBI221-carrying (i.e., vector control) protoplasts, GFP fluorescence were distributed throughout the protoplasts. In *p35S::PnF3H::GFP*-containing protoplasts, GFP signals were mainly distributed to the cytosol (Fig. 1i). When green fluorescence, bright field, and red fluorescence images were merged, distinct yellow signals were not detected in chloroplasts. These results suggested that PnF3H is a cytosol protein.

PnF3H enhanced the salinity tolerance and the antioxidant activity of transgenic *Arabidopsis*

Three homozygous *PnF3H* overexpressing lines (i.e., AtOE1, AtOE2, and AtOE3) were constructed and the gene expression levels of *PnF3H* were detected by RT-PCR method. For phenotype analysis, seeds from the wild-type plants and AtOE lines were sown on 1/2 MS agar medium supplemented with or without NaCl. In the absence of exogenous NaCl, there were no differences in the germination rates between the AtOE lines and the WT plants. However, following the 100 mM NaCl treatment, the germination rates of AtOE1, AtOE2, and AtOE3 plants were 56.3, 45.0, and 40.0%, respectively, which were higher than the 25.0% germination rate for the WT plants (Fig. 2a, c). In the presence of 125 mM NaCl, the germination rates of AtOE lines

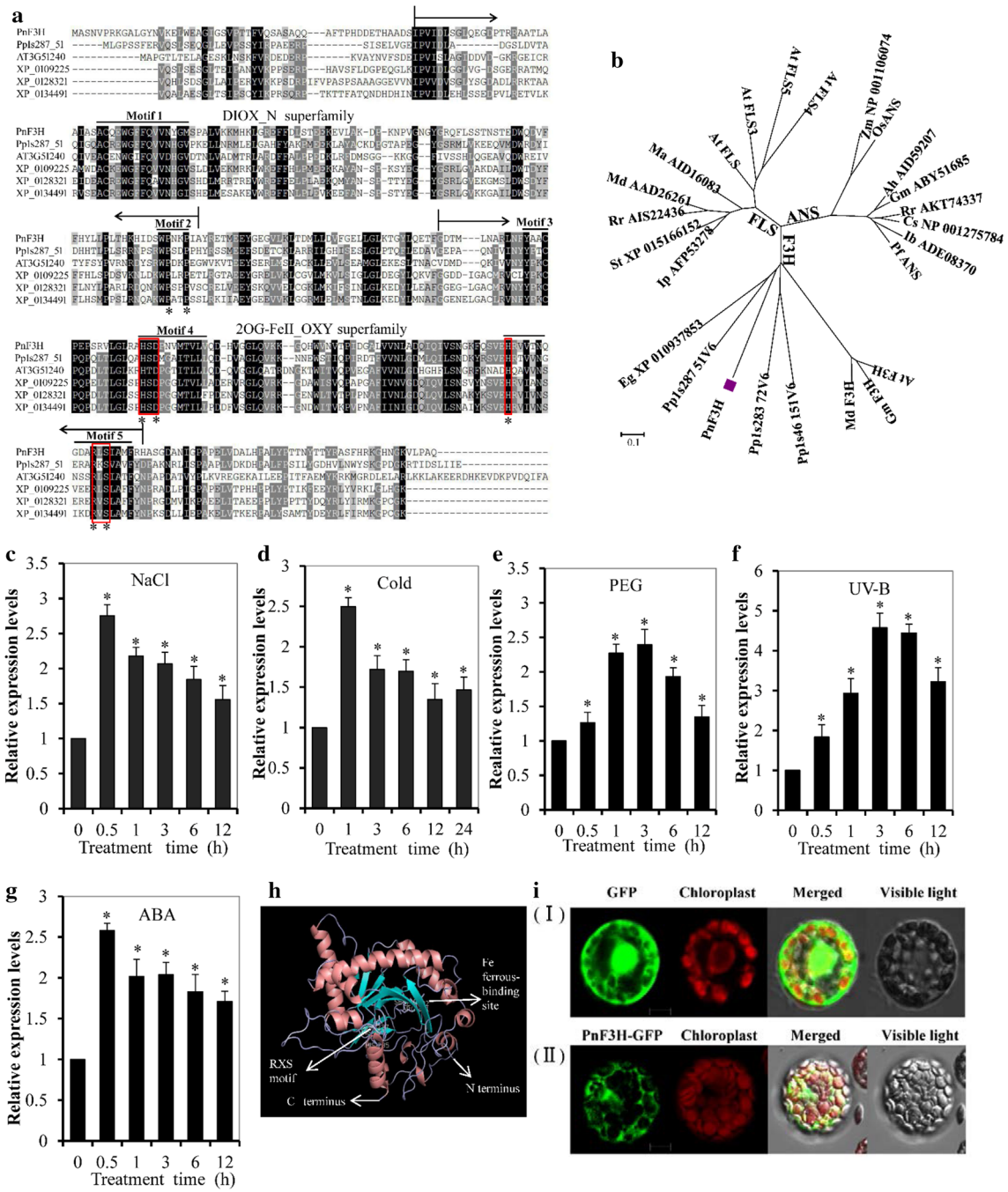

Fig. 1 PnF3H encodes an F3H protein and induced by various abiotic stresses. **a** Sequence alignment of PnF3H with other F3Hs. The positions of the five conserved motifs were labeled with *bold lines*. *Red frames* indicated the conserved motifs required for ferrous iron (HXD) and 2-oxoglutarate binding (RXS); *Asterisks* (*) indicated the conserved amino acid residues in F3Hs. **b** Phylogenetic tree was constructed using the neighbor-joining method. **(c–g)** PnF3H is induced by various abiotic stresses. **c** 200 mM NaCl treatment; **d** Cold treatment (4 °C); **e** 20% PEG6000 treatment for simulated drought stress. **f** UV-B radiation; **g** 50 μM abscisic acid (ABA) treatment. *Vertical bar* indicate mean ± SE of three replicates of the sample. *Asterisks* (*) indicate significant differences of means between the control group and the treatment group ($p < 0.05$). **h** 3-D structural model of PnF3H. The α-helix, β-sheet and random coils were colored with *salmon, cyan*, and *bright blue*, respectively. The conserved ferrous iron binding site HXDX55H (His^{233}, Asp^{235}, and His^{289}) and the 2-oxoglutarate (2-ODD) binding domain RXS (Arg^{299} and Ser^{301}) were *labeled by arrow*. **i** PnF3H protein targets to the cytosol. *Arabidopsis* protoplasts were transformed with *p35S::GFP*/pBI221 vectors (I) and *p35S::PnF3H::GFP*/ pBI221 (II). The confocal images were taken after 12 h of transfection. *Green fluorescence* of PnF3H-GFP or GFP proteins, *bright* field of protoplast, *red fluorescence* of chloroplasts and merged images were captured. *Bar* 10 μm. (Color figure online)

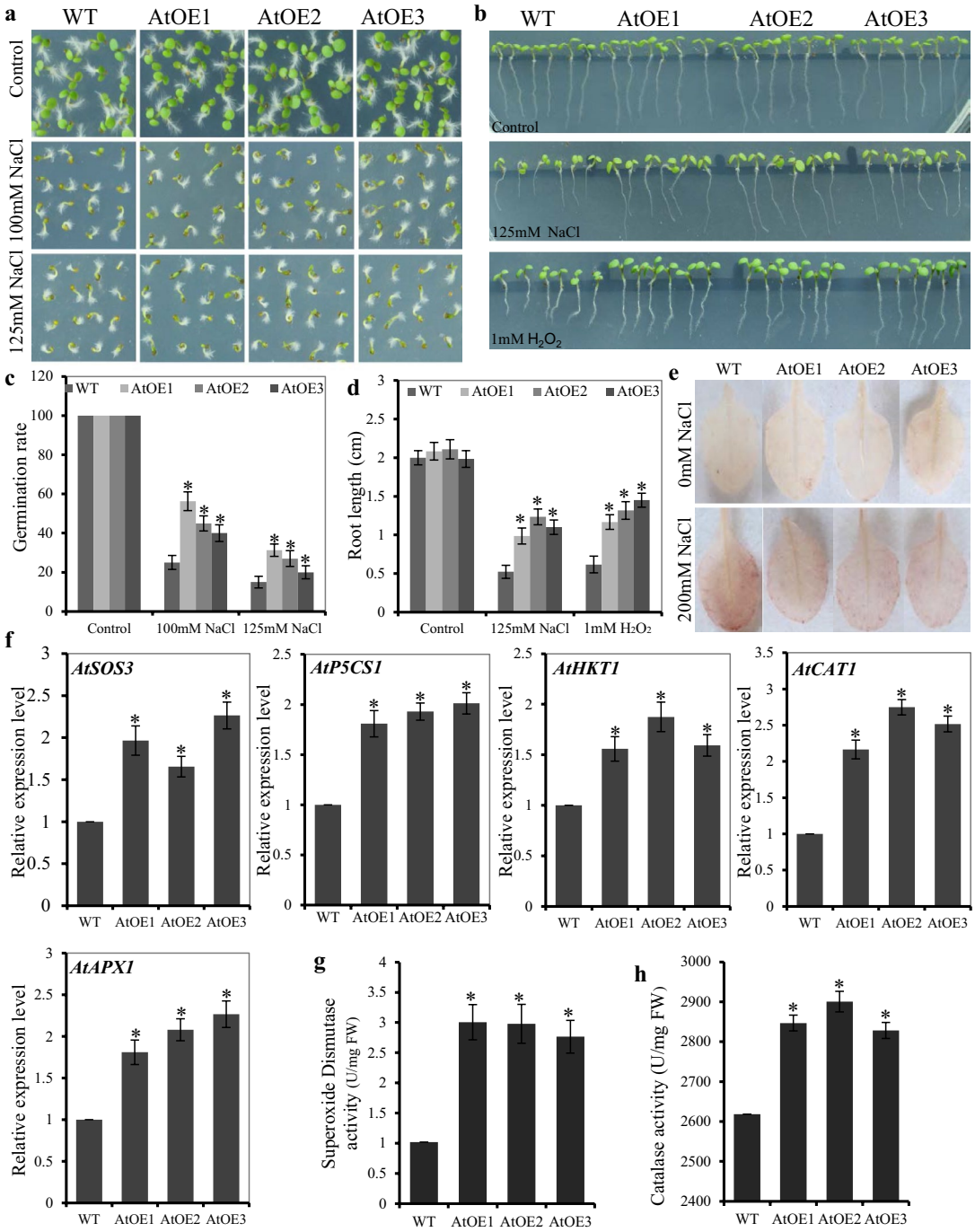

Fig. 2 PnF3H contributed to the salt- and oxidative- stress tolerance in transgenic *Arabidopsis*. **a** The seed germination rate of the AtOE lines was significantly higher than that of the WT plants under salt stress (6 days' seed germination). **b** Primary root length of *Arabidopsis* seedlings under salt- or oxidative- stress. **c** Statistical analysis of seed germination rates as shown in (**a**). **d** Statistical analysis of primary root length of *Arabidopsis* seedlings under salt- or oxidative-stress in (**b**). **e** ROS levels of *Arabidopsis* by DAB staining without salt treatment, and ROS levels of *Arabidopsis* by DAB staining with 200 mM NaCl treatment. **f** The expression levels of several stress resistance genes were analyzed by real-time PCR. **g** SOD and **h** CAT activities of 2-week-old *Arabidopsis* seedlings with 200 mM NaCl treatment. Data were presented as means ± SE, and *asterisks* (*) indicated significant differences of means between the AtOE lines and the WT plants ($P < 0.05$)

were also higher than that of the WT plants (Fig. 2c). For root growth assay, under normal conditions, no differences were observed between the WT plants and the AtOE lines (Fig. 2b). In the presence of 125 mM NaCl, the AtOE lines were more vigorous than the WT plants, forming longer primary roots.

Salt tolerance is usually related to oxidative stress responsive signaling pathway (Golldack et al. 2014). *PnF3H* overexpressing lines showed superior growth status comparing with the WT line in the presence of 1.0 mM H_2O_2. The root length of the transgenic plants was approximately twofold longer than that of the WT plants at 1/2 MS medium containing 1 mM H_2O_2 (Fig. 2d). DAB staining showed that signals in the AtOE lines were weaker than those in the WT plants (Fig. 2e), suggesting that the transgenic plants exhibited lower H_2O_2 level under NaCl treatment. Additionally, the activities of superoxide dismutase (SOD) and catalase (CAT) in the AtOE lines were higher than that in the WT plants after NaCl treatment (Fig. 2g, h).

To reveal the possible molecular mechanisms underlying the improvement of stress resistance in transgenic *Arabidopsis*, 2-day-old germinating seeds were subjected to 200 mM NaCl treatment. The expression levels of several stress responsive genes (i.e., *AtSOS3, AtP5CS1* and *AtHKT1*) in the AtOE lines and the WT plants were detected by real-time PCR. Under 200 mM NaCl treatment, the expression levels of those genes were up-regulated in the AtOE lines than that in the WT plants. Moreover, the expression levels of antioxidant enzymes (i.e., *AtCAT1* and *AtAPX1*) in PnF3H overexpression lines were also higher than that in the WT plants (Fig. 2f).

PnF3H decreased the ABA sensitivity in transgenic *Arabidopsis*

ABA is a vital stress response-associated phytohormone that responses to biotic and abiotic stresses (Verma et al. 2016). For germination assays, results showed that the AtOE lines were insensitive to the provision of exogenous ABA. In the absence of exogenous ABA, there were no obvious differences in the germination rates between the AtOE lines and the WT plants. Under ABA treatment, the germination of the AtOE lines and the WT plants were both significantly inhibited, while the germination rates of the AtOE lines were markedly higher than that of the WT plants (Fig. 3a). The germination rates of the AtOE lines, which were germinated 3 days after sowing at 0.5 μM ABA, were more than 75.0%, while the germination rates of the WT plants were approximately 31.2% (Fig. 3b). The germination rates after treating plants with 0.75 μM ABA were 37.5, 43.7, 52.5% for AtOE1, AtOE2, and AtOE3 plants, respectively, which were higher than that of the WT plants (18.7%) (Fig. 3b). For early root growth assay, under normal conditions, there were indistinguishable phenotypes between the WT plants and the AtOE lines (Fig. 3c). However, in the presence of 0.5 μM ABA or 0.75 μM ABA, the AtOE lines were more vigorous than the WT plants, forming longer primary roots (Fig. 3c).

To clarify the molecular mechanism mediating the ABA effects, germinated seeds were sprayed with 50 μM ABA or deionized water (control samples) 2 days after germination. Real-time PCR analysis showed that the transcription levels of ABA-responsive genes such as *AtABI3, AtABI4, AtABI5*, and *AtABF3* were substantially down-regulated in the AtOE lines when compared the WT plants, with respect to plants at 50 μM ABA treatment (Fig. 3f). Furthermore, by measuring the content of endogenous ABA in 2-week old plants, results showed that the ABA levels in the AtOE lines were lower than that in the WT plants (Fig. 3e). Thus, PnF3H inhibited the expression of ABA pathway which were related to the seed germination and seedling growth in transgenic plants.

Determination of PnF3H activity in transgenic plants

Plants were cultured in liquid MS medium in the absence or presence of 200 μM naringenin for 2 weeks respectively (Yun et al. 2008). Without naringenin treatment, there was no obvious difference in phenotypes between the AtOE plants and the WT plants (Fig. 4a). However, under 200 μM naringenin treatment, the root length of the AtOE lines were longer than that of the WT plants (Fig. 4a). Thus, overexpressing *PnF3H* could alleviate the inhibitive effects of naringenin on plant root growth. Moreover, flavonoids in the AtOE lines appeared new peaks under naringenin treatment when compared to the WT plants. PnF3H might play a key role in catalyzing naringenin to new products (Fig. 4 b and c, peaks P1 and P2).

Discussion

Flavonoids are a large family of plant phenolic pigments. Flavonoid biosynthesis pathway has been basically revealed through enzymologic studies in the model plant *Arabidopsis thaliana* (Saito et al. 2013). However, the secondary metabolic pathways in plants are extremely complex and each plant species has obviously distinctive profiles of flavonoids (Tu et al. 2016). Therefore, it is essential to identify species-specific genes in the flavonoid biosynthesis pathway. In this study, we carried out a sequence analysis of a flavanone 3-hydroxylase gene (i.e., *PnF3H*) from the Antarctic moss *P. nutans* and revealed its roles in abiotic stresses. Bioinformatics analysis suggested that PnF3H was highly homologous with F3Hs from other plants (Fig. 1a). F3H is classified under Fe^{II} and 2-ODD (Schofield and Zhang 1999). PnF3H also contained two conserved motifs: HxDxnH (His^{233}, Asp^{235}, and His^{289}) for binding Fe^{II} and RxS (Arg^{299} and

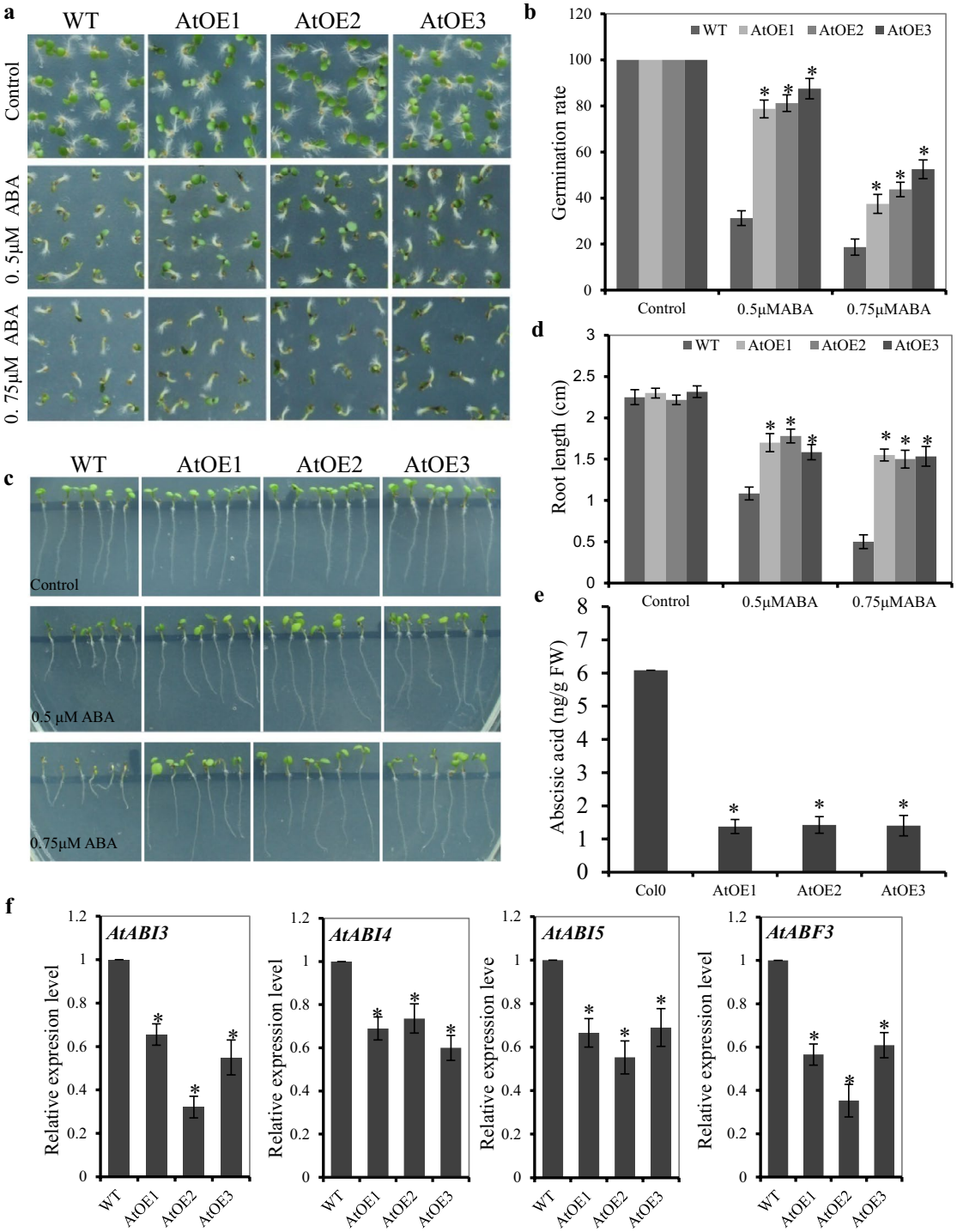

Fig. 3 PnF3H reduced the ABA sensitivity in transgenic *Arabidopsis*. **a** Seed germination in the AtOE lines were significantly higher than that in the WT plants under ABA treatment (3 days' seed germination). **b** Statistical analysis of the seed germination shown in (**a**). **c** PnF3H enhanced the primary root growth after ABA treatment. **d** Statistical analysis of the root length shown in (**c**). **e** Endogenous ABA content of 2-week-old *Arabidopsis* seedlings. **f** The expression levels of ABA-responsive genes were determined by real-time PCR. Tublin was used as an internal control. *Vertical bars* are means ± SE, and *asterisks* (*) indicate significant differences of means between the AtOE lines and the WT plants at $p < 0.05$

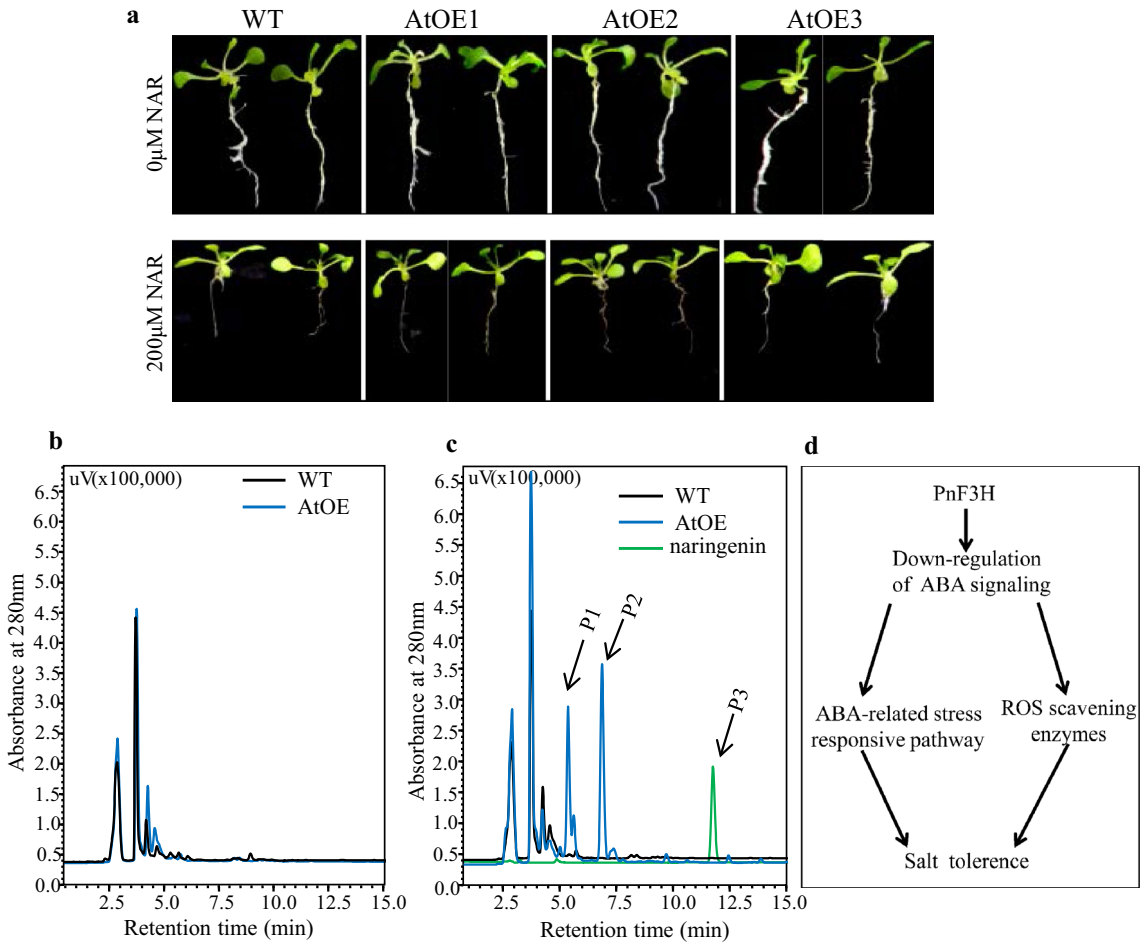

Fig. 4 Naringenin-feeding experiments and flavonoid metabolism profiling by HPLC analysis. **a** Surface-sterilized *Arabidopsis* seeds were cultured in liquid MS medium for 2 weeks with or without 200 μM naringenin (Sigma-Aldrich, USA). AtOE lines have growth superiority and alleviate the inhibition of naringenin on plant growth. **b** HPLC profile of total flavonoids of 2-week old *Arabidopsis* without 200 μM naringenin in liquid MS medium. **c** HPLC profile of total flavonoids of 2-week old *Arabidopsis* with 200 μM naringenin in liquid MS medium and 10 mM naringenin standard (Sigma-Aldrich, USA) monitored at 280 nm. **d** Hypothetical model of PnF3H function in abiotic stress

Ser^{301}) for binding 2-OG (2-oxoglutarate). Consistent with the diverse physiological functions, flavonoids are found in most plant cell compartments, including the cytosol, vacuole, chloroplast, nucleus, endoplasmic reticulum and the extracellular space (Zhao and Dixon 2010). Subcellular localization analysis showed that PnF3H located in cytosol (Fig. 1i).

Flavonoid biosynthesis enzyme, particularly flavanone 3-hydroxylase have been recently suggested as playing antioxidant functions in the responses of plants to a wide range of abiotic stresses. In the desert plant, *Reaumuria soongorica*, real-time PCR analysis showed that there was a rapid increase in gene expression of RsF3H under UV-B radiation and drought stress (Liu et al. 2013a). F3H is considered to be an important enzyme of flavonoid pathway leading to accumulation of flavan-3-ols in tea. Expression analysis revealed the upregulation of F3H transcripts (i.e., *CsF3H*) under salt stress (Mahajan and Yadav 2014). As show in Fig. 1, the transcript levels of PnF3H were also significantly increased under various treatments (i.e., high salinity, cold, 20% PEG6000, UV-B radiation or ABA).

Salt stress is one of the major abiotic factors (Hediye Sekmen et al. 2007). Flavonoids are involved in the restriction of salt-induced oxidative damages (Hamada AbdElgawad et al. 2016). For example, over-expression of a tea flavanone 3-hydroxylase gene (i.e., *CsF3H*) increased the content of flavan-3-ols and enhanced salt tolerance in transgenic tobacco (Mahajan and Yadav 2014). High salinity can also affect the growth of vegetation in Antarctica, as many species grow near the Antarctic coast. In this study, we found that overexpression of *PnF3H* improved plant tolerance to salinity stress with higher seeds germination rates and longer primary roots (Fig. 2). *P5CS* and *HKT1* are salt tolerance genes (Zhu 2001). P5CS encodes

Δ1-pyrroline-5-carboxylate synthetase, under the control of a stress-induced promoter AIPC (ABA-inducible promoter complex), confers tolerance to salt stress (Guerzoni et al. 2014). HKT1 encodes high-affinity K^+ transporter that facilitates Na^+ exclusion from root xylem. HKT1 and its functional variation are highly associated with salt tolerance (Mickelbart et al. 2015). In this study, the expression levels of *AtP5CS1* and *AtHKT1* were markedly higher in the AtOE lines than that in the WT plants (Fig. 2).

Abiotic stress usually leaded to accumulation of reactive oxygen species (ROS) and oxidative damage, plants resisted abiotic stress by scavenging the generation of reactive oxygen species (Liu et al. 2013a). Overexpression of anthocyanidin reductase from *rosa rugosa* (i.e., RrANR) in tobacco increased transcript expression and activity of several ROS-related and stress-responsive genes under chilling stress (Luo et al. 2016). The overexpression of a flavanone 3-hydroxylase from *Camellia sinensis* (i.e., CsF3H) enhanced the salt stress tolerance of the transgenic tobacco, and the result was accompanied with higher transcript expression level and activity of the antioxidant enzymes (Mahajan and Yadav 2014). In this study, the AtOE lines showed an obviously enhanced oxidative tolerance when compared to the WT plants (Fig. 3b). The result of DAB staining showed that the transgenic *Arabidopsis* plants had a lower H_2O_2 level (Fig. 2e). The AtOE lines also enhanced the gene expression levels and enzyme activities of ROS-scavenging enzymes under salt stress (Fig. 2f–h). Thus, PnF3H can contribute to reduce ROS level under abiotic stress.

Phytohormone ABA has been proposed to act as a pivotal regulator in regulating plant processes to resisting abiotic stresses, seed maturation, seed dormancy and plant development (Keskin et al. 2010). In tobacco, overexpression of *RrANR* enhances tolerance to abiotic stress via modulating ABA signaling (Luo et al. 2016). In this study, PnF3H transgenic *Arabidopsis* exhibited insensitivity to ABA in terms of seed germination and early root growth (Fig. 3a, c). Furthermore, the levels of endogenous ABA in the AtOE lines were also lower than that in the WT plants (Fig. 3e). Previously, molecular studies suggested that ABA signaling pathway might be conserved across land plant evolution (from mosses to higher plants) (Chater et al. 2013). For example, PpABI3 regulated ABA-responsible gene expression by interacting with the nuclear factor PpNF-Y in *P. patens* (Yotsui et al. 2013). In this study, the expression levels of genes (*AtABI3, AtABI4, AtABI5* and *AtABF3*) were decreased in transgenic *Arabidopsis* plants compared with the WT plants (Fig. 3f), which may be explained the reduced ABA sensitivity in transgenic *Arabidopsis*. Overall, these results suggested that PnF3H may serve as a flavonoid biosynthetic enzyme involving in regulating the salt tolerance and ABA sensitivity in *P. nutans*.

Naringenin is a precursor compound of flavonoids and the key substrate for flavonoids metabolism pathway (Yun et al. 2008; Du et al. 2010). Naringenin is taken up by *Arabidopsis* roots and can be catalyzed by flavanone-3-hydroxylase (F3H) into new flavonoids (Shirley et al. 1995). 1-*N*-naphthylphthalamic acid (NPA) is an auxin transport inhibitor. Naringenin is similar to NPA and can also inhibit auxin transport and then *Arabidopsis* root growth and gravitropism were inhibited (Brown et al. 2001; Yun et al. 2008). Overexpression flavone synthase (*FNS-I*) from *Petroselinum crispum* have no significant differences with the WT *Arabidopsis*. But, under naringenin-feeding condition, the *FNS-I* transgenic lines could accumulate substantial amounts of apigenin and alter the synthesis of flavones metabolize in transgenic *Arabidopsis*. In this study, naringenin-feeding experiment showed that AtOE lines also can alleviate the inhibitive effects of naringenin on plant growth and change flavonoid metabolism spectrum (Fig. 4). These results indicate that PnF3H has catalytic function in *Arabidopsis* and converts naringenin into new products.

Based on overall observations, the roles of PnF3H in enhancing salt stress tolerance and decreasing ABA sensitivity were proposed in Fig. 4d. Our proposition is that PnF3H down-regulates ABA signaling and further regulates the ABA-related stress responsive pathway and increases the level of ROS-scavenging activity, thereby explaining the positive effect of PnF3H on the salinity tolerance of *Arabidopsis*.

Acknowledgements This work was supported by the National Natural Science Foundation of China (41206176 and 41476174), Natural Science Foundation of Shandong Province (ZR2014DQ012), Basic Scientific Fund for National Public Research Institutes of China (2014T04), and Excellent Creative Team Fund of Jinan.

References

Agati G, Biricolti S, Guidi L, Ferrini F, Fini A, Tattini M (2011) The biosynthesis of flavonoids is enhanced similarly by UV radiation and root zone salinity in *L. vulgare* leaves. J Plant Physiol 168(3):204–212

Biasini M, Bienert S, Waterhouse A, Arnold K, Studer G, Schmidt T, Kiefer F, Gallo Cassarino T, Bertoni M, Bordoli L, Schwede T (2014) SWISS-MODEL: modelling protein tertiary and quaternary structure using evolutionary information. Nucleic Acids Res 42:W252–W258

Brown AM, Rashotte AS, Murphy, JN, Brian WT, Peer WA, Lincoln Taiz GKM (2001) Flavonoids act as negative regulators of auxin transport in vivo in *Arabidopsis*. Plant Physiol 126:524–535

Chater C, Gray JE, Beerling DJ (2013) Early evolutionary acquisition of stomatal control and development gene signalling networks. Curr Opin Plant Biol 16(5):638–646

Chen W, Gong L, Guo Z, Wang W, Zhang H, Liu X, Yu S, Xiong L, Luo J (2013) A novel integrated method for large-scale detection, identification, and quantification of widely targeted metabolites: application in the study of rice metabolomics. Mol Plant 6(6):1769–1780

Chen Q, Zhang X, Liu Y, Wei J, Shen W, Shen Z, Cui J (2017) Hemin-mediated alleviation of zinc, lead and chromium toxicity is associated with elevated photosynthesis, antioxidative capacity; suppressed metal uptake and oxidative stress in rice seedlings. Plant Growth Regul 81(1):253–264

Clarke LJ, Robinson SA (2008) Cell wall-bound ultraviolet-screening compounds explain the high ultraviolet tolerance of the Antarctic moss, *Ceratodon purpureus*. New Phytol 179(3):776–783

Czemmel S, Heppel SC, Bogs J (2012) R2R3 MYB transcription factors: key regulators of the flavonoid biosynthetic pathway in grapevine. Protoplasma 249(2):109–118

Du Y, Chu H, Wang M, Chu IK, Lo C (2010) Identification of flavone phytoalexins and a pathogen-inducible flavone synthase II gene (SbFNSII) in sorghum. J Exp Bot 61(4):983–994

Falcone Ferreyra ML, Rius SP, Casati P (2012) Flavonoids: biosynthesis, biological functions, and biotechnological applications. Front Plant Sci 3:222–237

Fu J, Sun X, Wang J, Yan C (2012) Simple rapid, and simultaneous assay of multiple carboxyl containing phytohormones in wounded tomatoes by using single SPE purification and isotope dilution. Anal Chem 28:1081–1087

Golldack D, Li C, Mohan H, Probst N (2014) Tolerance to drought and salt stress in plants: unraveling the signaling networks. Mol Genet Genom 5:151–161

Guerzoni JTS, Belintani NG, Moreira RMP, Hoshino AA, Domingues DS, Bespalhok Filho JC, Vieira LGE (2014) Stress-induced Δ1-pyrroline-5-carboxylate synthetase (P5CS) gene confers tolerance to salt stress in transgenic sugarcane. Acta Physiol Plant 36(9):2309–2319

Hamada AbdElgawad GZ, Hegab MM, Pandey R, Asard H, Abuelsoud W (2016) High salinity induces different oxidative stress and antioxidant responses in maize seedlings organs. Front Plant Sci 7:1–11

Hediye Sekmen A, Türkan İ, Takio S (2007) Differential responses of antioxidative enzymes and lipid peroxidation to salt stress in salt-tolerant *Plantago maritima* and salt-sensitive Plantago media. Physiol Plant 131(3):399–411

Keskin BC, Sarikaya AT, Yüksel B, Memon AR (2010) Abscisic acid regulated gene expression in bread wheat (*Triticum aestivum L.*). Aust J Crop Sci 4(8):617–625

Kumar S, Nei M, Dudley J, Tamura K (2008) MEGA: a biologist-centric software for evolutionary analysis of DNA and protein sequences. Brief Bioinform 9(4):299–306

Li J, Lv X, Wang L, Qiu Z, Song X, Lin J, Chen W (2017) Transcriptome analysis reveals the accumulation mechanism of anthocyanins in 'Zijuan' tea (*Camellia sinensis* var. *asssamica* (Masters) kitamura) leaves. Plant Growth Regul 81(1):51–61

Liu M, Li X, Liu Y, Cao B (2013a) Regulation of flavanone 3-hydroxylase gene involved in the flavonoid biosynthesis pathway in response to UV-B radiation and drought stress in the desert plant, *Reaumuria soongorica*. Plant Physiol Biochem 73:161–167

Liu S, Wang N, Zhang P, Cong B, Lin X, Wang S, Xia G, Huang X (2013b) Next-generation sequencing-based transcriptome profiling analysis of *Pohlia nutans* reveals insight into the stress-relevant genes in Antarctic moss. Extremophiles 17(3):391–403

Liu S, Wang J, Chen K, Zhang Z, Zhang P (2017) The L-type lectin receptor-like kinase (PnLecRLK1) from the Antarctic moss *Pohlia nutans* enhances chilling-stress tolerance and abscisic acid sensitivity in *Arabidopsis*. Plant Growth Regul 81:409–418

Livak KJ, Schmittgen TD (2001) Analysis of relative gene expression data using real-time quantitative PCR and the 2(−Delta Delta C(T)) Method. Methods 25(4):402–408

Luo P, Shen Y, Jin S, Huang S, Cheng X, Wang Z, Li P, Zhao J, Bao M, Ning G (2016) Overexpression of *Rosa rugosa* anthocyanidin reductase enhances tobacco tolerance to abiotic stress through increased ROS scavenging and modulation of ABA signaling. Plant Sci 245:35–49

Mahajan M, Yadav SK (2014) Overexpression of a tea flavanone 3-hydroxylase gene confers tolerance to salt stress and *Alternaria solani* in transgenic tobacco. Plant Mol Biol 85(6):551–573

Meng C, Zhang S, Deng YS, Wang GD, Kong FY (2015) Overexpression of a tomato flavanone 3-hydroxylase-like protein gene improves chilling tolerance in tobacco. Plant Physiol Biochem 96:388–400

Mickelbart MV, Hasegawa PM, Bailey-Serres J (2015) Genetic mechanisms of abiotic stress tolerance that translate to crop yield stability. Nat Rev Genet 16(4):237–251

Perez-Cano FJ, Castell M (2016) Flavonoids, inflammation and immune system. Nutrients 8(10):659

Saito K, Yonekura-Sakakibara K, Nakabayashi R, Higashi Y, Yamazaki M, Tohge T, Fernie AR (2013) The flavonoid biosynthetic pathway in *Arabidopsis*: structural and genetic diversity. Plant Physiol Biochem 72:21–34

Sankari SL, Babu NA, Rani V, Priyadharsini C, Masthan KMK (2014) Flavonoids-clinical effects and applications in dentistry: a review. J Pharm Bioallied Sci 6(Suppl 1):S26–S29

Schofield CJ, Zhang Z (1999) Structural and mechanistic studies on 2-oxoglutarate-dependent oxygenases and related enzymes. Curr Opin Struct Biol 9(6):722–731

Schroeter B, Green TGA, Kulle D, Pannewitz S, Schlensog M, Sancho LG (2012) The moss *Bryum argenteum var. muticum* Brid. is well adapted to cope with high light in continental Antarctica. Antarct Sci 24(03):281–291

Shirley BW, Kubasek WL, Storz G, Bruggemann E, Koornneef M, Ausubel FM, Goodman HM (1995) Analysis of *Arabidopsis* mutants deficient in flavonoid biosynthesis. Plant J 8(5):659–671

Singh J, Dubey AK, Singh RP (2010) Antarctic terrestrial ecosystem and role of pigments in enhanced UV-B radiations. Rev Environm Sci Biol 10(1):63–77

Skotnicki ML, Ninham JA, Selkirk PM (2004) Genetic diversity, mutagenesis and dispersal of Antarctic mosses—a review of progress with molecular studies. Antarct Sci 12(03):363–373

Tu Y, Liu F, Guo D, Fan L, Zhu Z, Xue Y, Gao Y, Guo M (2016) Molecular characterization of flavanone 3-hydroxylase gene and flavonoid accumulation in two chemotyped safflower lines in response to methyl jasmonate stimulation. BMC Plant Biol 16(1):132–144

Verma V, Ravindran P, Kumar PP (2016) Plant hormone-mediated regulation of stress responses. BMC Plant Biol 16(1):86–96

Wang J, Zhang P, Liu S, Cong B, Chen K (2016) A leucine-rich repeat receptor-like kinase from the Antarctic moss *Pohlia nutans* confers salinity and ABA stress tolerance. Plant Mol Biol Rep 34(6):1136–1145

Xiong S, Tian N, Long J, Chen Y, Qin Y, Feng J, Xiao W, Liu S (2016) Molecular cloning and characterization of a flavanone 3-hydroxylase gene from *Artemisia annua* L. Plant Physiol Biochem 105:29–36

Yotsui I, Saruhashi M, Kawato T, Taji T, Hayashi T, Quatrano RS, Sakata Y (2013) ABSCISIC ACID INSENSITIVE3 regulates abscisic acid-responsive gene expression with the nuclear factor Y complex through the ACTT-core element in *Physcomitrella patens*. New Phytol 199(1):101–109

Yu HQ, Han N, Zhang YY, Tao Y, Chen L, Liu YP, Zhou SF, Fu FL, Li WC (2017) Cloning and characterization of vacuolar H^+-pyrophosphatase gene (AnVP1) from *Ammopiptanthus nanus* and its heterologous expression enhances osmotic tolerance in yeast and *Arabidopsis thaliana*. Plant Growth Regul 81(3):385–397

Yun CS, Yamamoto T, Nozawa A, Tozawa Y (2008) Expression of parsley flavone synthase I establishes the flavone biosynthetic

pathway in *Arabidopsis thaliana*. Biosci Biotechnol Biochem 72(4):968–973

Zhang X, Henriques R, Lin SS, Niu QW, Chua NH (2006) Agrobacterium-mediated transformation of *Arabidopsis thaliana* using the floral dip method. Nat Protoc 1(2):641–646

Zhang P, Zhang Z, Wang J, Cong B, Chen K, Liu S (2014) A novel receptor-like kinase (PnRLK-1) from the Antarctic moss *Pohlia nutans* enhances salt and oxidative stress tolerance. Plant Mol Biol Rep 33(4):1156–1170

Zhao J, Dixon RA (2010) The 'ins' and 'outs' of flavonoid transport. Trends Plant Sci 15(2):72–80

Zhu JK (2001) Plant salt tolerance. Trends Plant Sci 6(2):66–71